Core polarization effects on spin-dipole and first-forbidden β-decay operators in the lead region

E. K. Warburton
Brookhaven National Laboratory, Upton, New York 11973
(Received 22 June 1990)

The effect of two-particle–two-hole ground-state correlations on spin-dipole transitions and the similar first-forbidden β-decay transitions is studied for nuclei in the lead region with realistic shell-model interactions. Transitions are considered between states for which one is a particle-hole excitation of the other. It is found that the tensor component of the residual interaction is quite important for the 0^- and 1^- spin-dipole transitions and the analogous β-decay matrix elements. It is destructive for 0^- and constructive for 1^- so that the quenching of the two modes is quite different. The atypical $1g_{9/2} \rightarrow 0h_{9/2}$ transition is described. The results are compared to previous determinations.

I. INTRODUCTION

There is current interest in the excitation of collective states with $J^\pi = 0^-$, 1^-, and 2^- via the transition operators[1]

$$T_{\lambda\mu} = \sum_i \mathbf{r}_i [Y_{l=1}(\hat{\mathbf{r}}_i) \otimes \sigma_i]_{\lambda\mu} \tau_{\pm 1}, \quad \lambda = 0^-, 1^-, 2^-. \tag{1}$$

These are referred to as spin-dipole transition operators and, in a compact notation, are also written[2] as $[\mathbf{r}, \boldsymbol{\sigma}]^R$, where R (= 0, 1, 2) is the rank of the operator. The three $[\mathbf{r}, \boldsymbol{\sigma}]^R$ operators comprise half of the set responsible for first-forbidden β decay which proceeds in normal order through these three operators and, in addition, via the rank-zero operator γ_5 and the rank-one operators $\mathbf{r}$ and $\boldsymbol{\alpha}$.[2] Evaluation of the matrix elements of the six β-decay operators is also of much current interest because of the strong mesonic enhancement of the matrix element of γ_5.[3–6,2] That is, appraisal of this enhancement is aided by an understanding of the whole transition process. It is well known that first-order contributions from excitations of the core have a potentially large effect on the matrix elements of these six operators.[7–10,5,11,12] The important core-excited admixtures in the initial (final) state are those connected by a one-body operator to the dominant terms in the final- (initial-) state wave function. It is usually impossible to perform a shell-model diagonalization in a large enough Hilbert space to include all these effects. This is always true for the lead region. Thus it is customary to include the effects of such terms from outside the model space via effective operators. Because the admixtures in question are often a very small part of the wave function, this is potentially a very accurate procedure. The purpose of this article is to describe an evaluation of these effective operators for $Z \leq 82$ nuclei in the lead region using first-order perturbation theory within the confines of the spherical shell model.

II. CALCULATIONS

A conventional notation for the matrix elements of the six beta-decay operators is M_0^S, u, and z for the $R = 0, 1, 2$ components of $[\mathbf{r}, \boldsymbol{\sigma}]^R$, and M_0^T and x for the matrix elements of γ_5 and $\mathbf{r}$. The matrix element of $\boldsymbol{\alpha}$ can be related to that of $\mathbf{r}$ by the conserved-vector-current hypothesis or some other less-rigorous means[2] and need not be considered further. The notation M_0^S and M_0^T reminds us that these two matrix elements are of rank zero and are the space and time components of the axial current.[3,10,2]

We will discuss the specific case of first-forbidden β^- decay. The results are equally applicable to the n $\rightarrow$ p charge-exchange process and the inverse p $\rightarrow$ n charge-exchange on the final state so that both τ_{-1} and τ_{+1} excitations [see Eq. (1)] are considered. The applicability of the results is limited by the choice of orbits considered. The orbits nearest the Fermi surface for $A \sim 208$ nuclei are shown schematically in Fig. 1. With the active orbits shown in this figure it is presently possible to perform shell-model calculations which involve 1p-1h excitations relative to ^{208}Pb and which are otherwise unrestricted; for instance, Poppelier and Glaudemans[13] treated many nuclei in the $A \sim 208$ region in this manner with a surface-delta interaction (SDI) in this model space — which we therefore refer to as the PG model space. Thus, we are mainly concerned here with contributions from outside the PG model space. The specific example of ^{206}Tl $\rightarrow$ ^{206}Pb decay is shown schematically in Fig. 2. This is our prototype transition. In Fig. 2, the dominant configurations are shown at the top and an example of a 1p-1h admixture in the initial state and a 2p-2h admixture (final-state correlation) in the final state are shown at the bottom. We will treat admixtures perturbatively. Other more ambitious approaches — such as the random-phase-approximation (RPA) and finite-Fermi-systems approaches discussed by Ejiri and Fujita[11] and by Krmpotic, Ebert, and Wild[12]

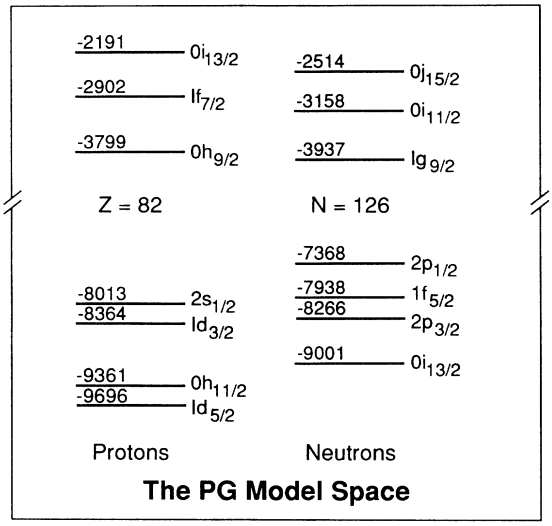

FIG. 1. The Poppelier-Glaudemans (PG) model space for the lead region. Single-particle energies (in MeV) are taken from the experimental spectra of $A = 207$ and 209 nuclei and are relative to ^{208}Pb.

— add additional admixtures from core excitations that do not connect in first order to the dominant pieces of the wave functions and thus contribute in orders higher than the first. The uncertainties generated by making these higher-order corrections (presumed small) may well be larger than the corrections themselves; thus, we direct our attention to first-order corrections only. We follow the approach of Towner *et al.*[8–10,14] Restrictions on the matrix elements of **r** and its derivatives limits first-forbidden decay to transitions between adjacent major shells. That is, specifying the major shell by the quantum number Q [$Q = 2N + l$, where N is the principal quantum (= 0,1,...) and l is the orbital angular momentum], the transitions are limited by the selection rule $\Delta Q = \pm 1$. The orbits which can contribute are listed in Table I where they are grouped into major shells.

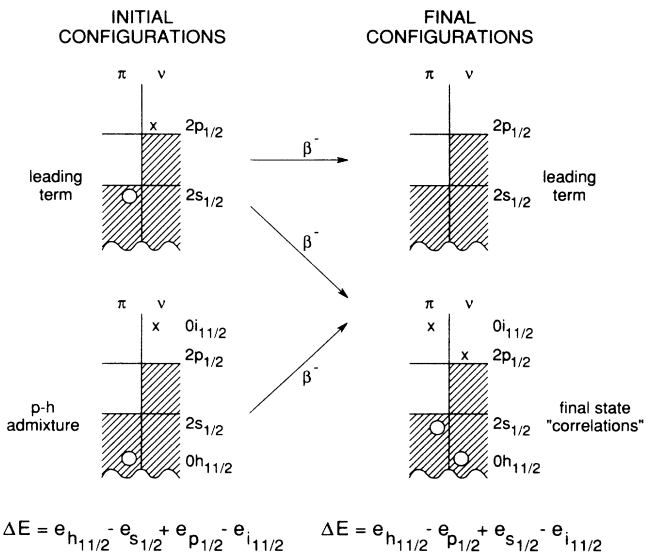

FIG. 2. Diagram indicating some of the relevant configurations entering for first-forbidden transitions in the lead region. The example shown is that of ^{206}Tl → ^{206}Pb. Arrows indicate the configurations linked by the beta decay.

The $\Delta Q = \pm 1$ selection rule and Pauli blocking due to the large neutron excess severely restricts the contributions from initial-state admixtures for the lead region. We shall restrict our discussion to transitions connecting the three neutron orbits below and the two above the $N = 126$ shell closure to the four proton orbits below and the one above the $Z = 82$ shell closure. The only contributing initial-state admixtures will be those involving holes in the unique-parity $Q = 5$ $0h_{11/2}$ proton orbit and, with the exception of the rank-two $\nu 1g_{7/2} \rightarrow \pi 0h_{11/2}$ transition, all are included in the PG model space and thus need not be added perturbatively. Examples of the effect of initial-state admixtures on the leading term, $\nu 2p_{1/2} \rightarrow \pi 2s_{1/2}$, in ^{206}Hg($0^+$) → ^{206}Tl($0^-$) and

TABLE I. Neutron single-particle energies used in the pertubative treatment of core excitation. The results for orbits 17–29,31 are from single-neutron transfer reactions as compiled in Fig. 1 of Zwarts and Glaudemans (Ref. 15). For orbits 12–16 neutron single-particle energies were obtained by subtracting 7.058 MeV from the proton single-particle energies listed in Ref. 15. This is the average difference between the proton and neutron energies for orbits 17–22. The values for orbits 11, 30, and 32 are based on the systematics of spin-orbit energy splittings. The orbits are grouped into major shells.

Orbit No.	Orbit	E_{orbit} (MeV)
$Q = 4$		
11	$0g_{9/2}$	−21.539
12	$0g_{7/2}$	−18.539
13	$1d_{5/2}$	−16.739
14	$1d_{3/2}$	−15.416
15	$2s_{1/2}$	−15.065
$Q = 5$		
16	$0h_{11/2}$	−16.406
17	$0h_{9/2}$	−10.781
18	$1f_{7/2}$	−9.708
19	$1f_{5/2}$	−7.937
20	$2p_{3/2}$	−8.265
21	$2p_{1/2}$	−7.368
$Q = 6$		
22	$0i_{13/2}$	−9.001
23	$0i_{11/2}$	−3.157
24	$1g_{9/2}$	−3.936
25	$1g_{7/2}$	−1.445
26	$2d_{5/2}$	−2.369
27	$2d_{3/2}$	−1.398
28	$3s_{1/2}$	−1.904
$Q = 7$		
29	$0j_{15/2}$	−2.513
30	$0j_{13/2}$	+6.000
31	$1h_{11/2}$	−0.634
32	$1h_{9/2}$	+5.000

TABLE II. Contributions to the matrix elements M_0^S and M_0^T from the possible single-particle transitions in $^{206}\mathrm{Hg}(0^+) \rightarrow ^{206}\mathrm{Tl}(0^-) \rightarrow ^{206}\mathrm{Pb}(0^+)$ decay. The matrix elements are in fm and were calculated using the 1p-1h SDI interaction of Poppelier and Glaudemans (Ref. 13).

Orbit		$^{206}\mathrm{Hg} \rightarrow ^{206}\mathrm{Tl}$		$^{206}\mathrm{Tl} \rightarrow ^{206}\mathrm{Pb}$	
ν	π	M_0^S	M_0^T	M_0^S	M_0^T
$2p_{1/2}$	$2s_{1/2}$	−4.507	+58.804	−5.792	+75.568
$2p_{3/2}$	$1d_{3/2}$	−1.603	+20.913	−0.661	+8.624
$1f_{5/2}$	$1d_{5/2}$	−0.402	+5.249	−0.977	+12.747
$0i_{11/2}$	$0h_{11/2}$	+1.839	−23.991	+1.795	−23.419
$1g_{9/2}$	$0h_{9/2}$	−0.085	+1.105	−0.049	+0.639
Total		−4.758	+62.080	−5.684	+74.159

$^{206}\mathrm{Tl}(0^-) \rightarrow ^{206}\mathrm{Pb}(0^+)$ β^- decays are shown in Table II. These were calculated with the Poppelier-Glaudemans[13] 1p-1h SDI interaction using harmonic-oscillator (HO) wave functions. It is seen that the effect of the $\nu 0i_{11/2} \rightarrow \pi 0h_{11/2}$ admixed transition is large but need not be considered perturbatively.

By contrast, there are many possible $\Delta Q = \pm 1$ transitions involving the 2p-2h admixtures in the final state and from a practical point of view these can only be added perturbatively. For the $A \sim 208$ nuclei considered here these $\nu \rightarrow \pi$ transitions are in the sets $Q = 4 \rightarrow Q = 5$, $Q = 5 \rightarrow Q = 6$, and $0i_{13/2}(Q = 6) \rightarrow Q = 5$(*R*2 only), 7.

A given transition matrix element is formulated as a sum of one-body-transition densities (OBTD) times single-particle matrix elements. The OBTD contain the information on the nuclear structure of the initial and final states as determined by the model space and interaction used. It is then natural and customary to incorporate effects from outside the model space into *effective* single-particle matrix elements. We define the effective matrix element for a transition between a neutron in orbit m and a proton in orbit i for a first-forbidden operator S_J^α of rank J by

$$\langle j_i || S_J^\alpha || j_m \rangle_{\mathrm{eff}} = q_\alpha(j_m \rightarrow j_i) \langle j_i || S_J^\alpha || j_m \rangle_{\text{shell model}}, \tag{2}$$

where, in an obvious notation, $\alpha = S, u, z, T, x$. In first-order, the final-state "correlations" of Fig. 2 will give rise to a quenching factor of

$$q_\alpha(j_m \rightarrow j_i) = 1 - \sum_{nj} y_{nj,mi}, \tag{3}$$

where the 2p-2h admixtures in the final state have particles in the πn and νm orbits and holes in the πi and νj orbits *relative to the vacuum defined as the leading term of the final state.* Then, generalizing the results of Ref. 10,

$$y_{nj,mi} = (-)^{pr} \frac{B_{nj,mi}}{\Delta E_{nj,mi}} \frac{\langle 0 || S_J^\alpha || j_j^{-1} j_n; JT \rangle}{\langle 0 || S_J^\alpha || j_i^{-1} j_m; JT \rangle}, \tag{4}$$

where $\langle 0 || S_J^\alpha || j_i^{-1} j_m; JT \rangle$, the dominant term, is the matrix element of S_J^α between a final state, defined as the closed shell (vacuum) and an initial $j_m^{-1} j_i$ particle-hole excitation of the final state coupled to J with $T = 1$. The phase factor $(-)^{pr}$ originates in the definition of the Hermitian conjugation for the operator S_J^α; with our definition of the operators,[2] it is odd for M_0^T and the rank-one operator x and even otherwise.

The energy denominator $\Delta E_{nj,mi}$ is defined such as to be negative and is approximated by

$$\Delta E_{nj,mi} = e_j - e_m + e_i - e_n, \tag{5}$$

where the e_k are the single-particles energies (SPE) of the orbits involved. The single-particle energies used are listed in Table I. In Eq. (4), $B_{nj,mi}$ is precisely the B matrix of standard RPA theory as defined, e.g., by Towner (Eq. 4.54 of Ref. 14) and, in present notation is

$$B_{nj,mi} = [(1 + \delta_{mn})(1 + \delta_{ij})]^{1/2} (-)^{j_n + j_i + J} \times \sum_{J_1 T_1} (-)^{J_1 + T_1} \hat{J}_1^2 \hat{T}_1^2 W(\tfrac{1}{2}\tfrac{1}{2}\tfrac{1}{2}\tfrac{1}{2}; T_1 1) W(j_m j_n j_i j_j; J_1 J) \langle j_m j_n; J_1 T_1 | V | j_i j_j; J_1 T_1 \rangle, \tag{6}$$

where $\hat{j} = (2j+1)^{1/2}$, the W are Racah coefficients, and the last term is an antisymmetrized $2\hbar\omega$ two-particle matrix element. A similar first-order perturbation expression for the effect of admixtures in the initial state is given explicitly by Towner and Hardy.[9,16]

The $q_\alpha(j_m \rightarrow j_i)$ of Eq. (3) were evaluated for all possible transitions (see Fig. 1) between the neutron orbits $m = 2p_{1/2}, 1f_{5/2}, 2p_{3/2}, 1g_{9/2}, 0i_{11/2}$ and the proton orbits $i = 2s_{1/2}, 1d_{3/2}, 1d_{5/2}, 1h_{11/2}$ and for the $\nu 1g_{9/2} \rightarrow \pi 0h_{9/2}$ transition. The evaluation was made for five different residual interactions, two purely central interactions and three derived from nucleon-nucleon po-

tentials. The central interactions are the 1p-1h + 2p-2h (POP) SDI interaction of Poppelier and Glaudemans[13] already referred to, and the interaction of Gillet, Green, and Sanderson[18] (CAL). The interactions derived from G-matrix descriptions of nucleon-nucleon potentials are those of Hosaka, Kubo, and Toki[19] (H7B), which is based on the Paris[20] nucleon-nucleon potential. The earlier potentials of Anantaraman, Toki, and Bertsch[21] (P4Y) and Bertsch *et al.*[22,23] (M3Y) are based on the Paris and on the Hamada-Johnston[24] and Reid[25] nucleon-nucleon potentials, respectively.[26] The evaluations of these potentials were made using harmonic-oscillator wave functions, while the calculation of the single-particle matrix elements in Eq. (4) was made for both harmonic-oscillator and Woods-Saxon (WS) wave functions. For the latter we use the Woods-Saxon parameters of Streets, Brown, and Hodgson[27] which reproduce the experimental rms charge radius of ^{208}Pb of 5.503(2) fm and gives a neutron rms radius 0.2 fm larger. With normal shell occupancies, these radii correspond to $\hbar\omega = 6.701$ and 7.183 MeV for protons and neutrons, respectively. The average of these values of $\hbar\omega$ is 6.943 MeV. Thus this value (or one close to it) was used in all the calculations with HO wave functions.

III. RESULTS

As a first orientation to the results, we show in Table III values of $\sum_{n,j} y_{nj,mi}$ for the transitions $m = 2p_{1/2}, i = 2s_{1/2}$ in rank-zero and rank-one decay and $m = 2p_{1/2}, i = 1d_{3/2}$ in rank-two decay. These are the dominant transitions for ^{206}Tl decay and many other decays for $A = 205$–209 nuclei. The number of terms contributing to the sum in Eq. (3) is $12(R = 0)$, $33(R = 1)$, and $41(R = 2)$. We first note that the 2p-2h admixtures which contribute to the processes in first order are predicted to be very small. Thus a perturbative approach is well justified even though the effect of the admixtures can be very large. In principle, a correction should be made for the partial occupancy of orbits in

TABLE III. The first-order perturbative quenching factor $\sum_{n,j} y_{nj,mi}$ calculated with HO radial matrix elements and five different residual interactions for the rank-zero and rank-one $\nu 2p_{1/2} \rightarrow \pi 2s_{1/2}$ transitions and the rank-two $\nu 2p_{1/2} \rightarrow \pi 1d_{3/2}$ transition. The origin of the five interactions is discussed in the text.

Interaction	2p-2h (%)	$\sum_{n,j} y_{nj,mi}$ Total	Central	LS	Tensor
			$[\mathbf{r},\sigma]^0$ (M_0^S), $2p_{1/2} \rightarrow 2s_{1/2}$		
POP	0.39	0.4479	0.4479		
CAL	0.17	0.2593	0.2593		
H7B	0.26	0.0764	0.3814	0.0000	−0.3050
P4Y	0.22	0.0977	0.3641	0.0022	−0.2665
M3Y	0.26	0.1013	0.3900	0.0001	−0.2887
			$[\mathbf{r},\sigma]^1$ (u) , $2p_{1/2} \rightarrow 2s_{1/2}$		
POP	0.74	0.4648	0.4648		
CAL	0.30	0.2702	0.2703		
H7B	0.74	0.5536	0.3929	0.0041	0.1566
P4Y	0.67	0.5181	0.3745	0.0065	0.1372
M3Y	0.80	0.5573	0.4037	0.0051	0.1485
			x , $2p_{1/2} \rightarrow 2s_{1/2}$		
POP	0.74	0.6908	0.6908		
CAL	0.30	0.3466	0.3466		
H7B	0.74	0.3799	0.3657	0.0043	0.0099
P4Y	0.67	0.3513	0.3337	0.0091	0.0084
M3Y	0.80	0.4178	0.4002	0.0084	0.0091
			$[\mathbf{r},\sigma]^2$ (z) , $2p_{1/2} \rightarrow 1d_{3/2}$		
POP	0.39	0.5964	0.5964		
CAL	0.06	0.2201	0.2201		
H7B	0.14	0.2842	0.3256	0.0091	−0.0505
P4Y	0.13	0.3011	0.3113	0.0059	−0.0162
M3Y	0.14	0.3221	0.3306	−0.0002	−0.0086

TABLE IV. The first-order perturbative quenching factor $\sum_{n,j} y_{nj,mi}$ calculated with the H7B residual interaction with both HO and WS radial matrix elements.

Transition	HO	WS
	M_0^S(rank-zero)	
$2p_{1/2} \rightarrow 2s_{1/2}$	+0.0764	+0.0771
$2p_{3/2} \rightarrow 1d_{3/2}$	−0.0143	−0.0155
$1f_{5/2} \rightarrow 1d_{5/2}$	+0.1310	+0.1289
$0i_{11/2} \rightarrow 0h_{11/2}$	+0.1552	+0.1574
	M_0^T(rank-zero)	
$2p_{1/2} \rightarrow 2s_{1/2}$	−0.0764	−0.0814
$2p_{3/2} \rightarrow 1d_{3/2}$	+0.0143	+0.0077
$1f_{5/2} \rightarrow 1d_{5/2}$	−0.1310	−0.1376
$0i_{11/2} \rightarrow 0h_{11/2}$	−0.1552	−0.1520
	u(rank-one)	
$2p_{1/2} \rightarrow 2s_{1/2}$	+0.5536	+0.5297
$2p_{1/2} \rightarrow 1d_{3/2}$	+0.4674	+0.4562
$2p_{3/2} \rightarrow 2s_{1/2}$	+0.5985	+0.5836
$2p_{3/2} \rightarrow 1d_{3/2}$	+0.5200	+0.5247
$2p_{3/2} \rightarrow 1d_{5/2}$	+0.5501	+0.5182
$1f_{5/2} \rightarrow 1d_{3/2}$	+0.6878	+0.6600
$1f_{5/2} \rightarrow 1d_{5/2}$	+0.5521	+0.5244
$1g_{9/2} \rightarrow 0h_{11/2}$	+0.3555	+0.3364
$0i_{11/2} \rightarrow 0h_{11/2}$	+0.4015	+0.3999
	x(rank-one)	
$2p_{1/2} \rightarrow 2s_{1/2}$	+0.3799	+0.3614
$2p_{1/2} \rightarrow 1d_{3/2}$	+0.3083	+0.3004
$2p_{3/2} \rightarrow 2s_{1/2}$	+0.3887	+0.3789
$2p_{3/2} \rightarrow 1d_{3/2}$	+0.2391	+0.2480
$2p_{3/2} \rightarrow 1d_{5/2}$	+0.3654	+0.3457
$1f_{5/2} \rightarrow 1d_{3/2}$	+0.4478	+0.4290
$1f_{5/2} \rightarrow 1d_{5/2}$	+0.4550	+0.4210
$1g_{9/2} \rightarrow 0h_{11/2}$	+0.2206	+0.2126
$0i_{11/2} \rightarrow 0h_{11/2}$	+0.4305	+0.4058
	z(rank-two)	
$2p_{1/2} \rightarrow 1d_{3/2}$	+0.3158	+0.2889
$2p_{1/2} \rightarrow 1d_{5/2}$	+0.3672	+0.3411
$2p_{3/2} \rightarrow 2s_{1/2}$	+0.5679	+0.5509
$2p_{3/2} \rightarrow 1d_{3/2}$	+0.4702	+0.4842
$2p_{3/2} \rightarrow 1d_{5/2}$	+0.3920	+0.3737
$1f_{5/2} \rightarrow 1d_{3/2}$	+0.5802	+0.5475
$1f_{5/2} \rightarrow 1d_{5/2}$	+0.5841	+0.5580
$1g_{9/2} \rightarrow 0h_{11/2}$	+0.1718	+0.1572
$0i_{11/2} \rightarrow 0h_{11/2}$	+0.3685	+0.3737

specific cases. However, in practice, it is found that for the $A = 205$–209 nuclei under consideration, this correction is negligible compared to other uncertainties. Thus it was assumed that all orbits below doubly closed ^{208}Pb were full and all above were empty (an exception is made for the $\nu 1g_{9/2} \rightarrow \pi 0h_{9/2}$ transitions as discussed in Sec. IV B).

The two central interactions are included in Table III in order to illustrate the disparity that can exist between the results obtained with such schematic interactions. One should bear in mind that although the SDI interaction has been shown to be startlingly successful in describing nuclei in the lead region[13,15,28] it owes a large part of its success to the fact that it is a good representation of the total "bare + renormalization" interaction. Thus its use is not well justified here where the model space is, in principle, not truncated. The CAL interaction was included here because it was recently used in a similar treatment of quenching in neutrino capture by ^{205}Tl.[29] It is clear from examination of Table III that the omission of a tensor component from the POP and CAL interactions is a serious deficiency for the present application.

The three G-matrix interactions give essentially indistinguishable results. This was expected because, on the average, the two-particle matrix elements that appear in Eq. (6) are in fairly good agreement for the three potentials. For cases where a comparison can be made, they are also in close agreement with the bare G-matrix results of Kuo and Herling,[30] which are derived by the method of Kuo and Brown,[31] which is inherently more accurate than the potential representations of the interactions we consider. We shall only consider the H7B interaction in the rest of this discussion. It is seen that the tensor contribution to the quenching of M_0^S and u is quite appreciable. This was expected. Recall that Towner and Khanna,[10] in their study of the role of 2p-2h admixtures in ^{16}N(0^-) $\rightarrow$ ^{16}O(0^+) β^- decay, found that with realistic residual interactions the tensor contribution actually is dominant so that $q_S(2s_{1/2} \rightarrow 2p_{1/2})$ is larger than unity for this transition. Furthermore, Sagawa and Brown[1] considered the relative contributions

TABLE V. The first-order perturbative quenching factor $\sum_{n,j} y_{nj,mi}$ calculated for the $\nu 1g_{9/2} \rightarrow \pi 0h_{9/2}$ transition with HO and WS radial matrix elements and the H7B residual interaction.

Matrix element	HO/WS	Central	LS	Tensor	Total	$10\Delta_n$[a]
M_0^S	HO	+0.2056	+0.0000	−0.4226	−0.2170	−0.0522
	WS	+0.2368	+0.0000	−0.5224	−0.2856	−0.0723
M_0^T	HO	−0.2056	+0.0000	+0.4226	+0.2170	+0.0522
	WS	−0.1796	+0.0000	+0.3479	+0.1683	+0.0399
u	HO	+0.2127	+0.0044	+0.2246	+0.4398	−0.0298
	WS	+0.2472	+0.0067	+0.2777	+0.5317	−0.0420
x	HO	+0.0470	+0.0443	−0.0543	+0.0370	+0.2776
	WS	+0.0073	+0.0754	−0.0724	+0.0101	+0.3911
z	HO	+0.2254	+0.0003	−0.0762	+0.1586	
	WS	+0.2653	+0.0003	−0.0783	+0.1874	

[a]For occupancy of the $\nu 1g_9/2$ orbit in the initial state by $n(1g\frac{9}{2})$ neutrons, $\sum_{n,j} y_{nj,mi}$ is given by the value listed plus $\Delta_n n(1g\frac{9}{2})$.

to $\sum_{n,j} y_{nj,mi}$ in a study of the effect of 2p-2h admixtures on the $^{12}C(p,n)^{12}N(0^-,1^-,2^-)$ reaction. They present arguments, due to Mottelson,[32] showing that, in general, the tensor contribution should be in the approximate ratio $-\sqrt{20}$, $+\sqrt{15}$, and -1 for the matrix elements of $[\mathbf{r},\boldsymbol{\sigma}]^R$ with $R=0,1,2$, respectively, i.e., for M_0^S, u, and z. This expectation is in quantitative agreement with the results of Table III. They also found the LS contribution to be small. This general effect is also encountered in high-spin magnetic transitions.[33] The large contribution from the tensor component of the interaction means that results derived for $[\mathbf{r},\boldsymbol{\sigma}]^0$ and $[\mathbf{r},\boldsymbol{\sigma}]^1$ without the inclusion of a carefully considered tensor component are of little value.

The factor $\sum_{n,j} y_{nj,mi}$ for M_0^T is not included in Table III because for HO wave functions it is just the negative of that for M_0^S.[2] This is not true for Woods-Saxon wave functions, but, as we shall see, it is usually closely so.

In Table IV we collect $\sum_{n,j} y_{nj,mi}$ $[\equiv 1-q_\alpha(j_m \rightarrow j_i)]$ results for all $\nu(Q=5) \rightarrow \pi(Q=4)$ transitions which are possible in the model space of Fig. 1 and some $\nu(Q=6) \rightarrow \pi(Q=5)$ transitions. Results are shown for both HO and WS wave functions. Some additional results for the $\nu 1g_{9/2} \rightarrow \pi 0h_{9/2}$ transition are summarized in Table V.

IV. SUMMARY AND COMPARISON TO OTHER RESULTS

A. The results of Table IV

WS vs HO wave functions. The WS and HO results are in close agreement. This is not necessarily true for individual transitions but is partially a consequence of the averaging resulting from the summing of all possible contributions. The agreement is also a consequence of choosing the HO value of $\hbar\omega$ carefully as explained above.

The single-particle dependence of the quenching. There is clearly a dependence of q_α on $j_m \rightarrow j_i$. Thus, when possible, a different $q_\alpha(j_m \rightarrow j_i)$ should be used with each α, j_m, j_i. As an example of the application of the $q_\alpha(j_m \rightarrow j_i)$ of Table IV, we apply it to the M_0^S matrix element of the $^{206}Tl(0^-) \rightarrow {}^{206}Pb(0^+)$ transition of Table II and find a quenching of 0.95. In some applications use of an average or effective value of q_α could be a good enough approximation such as if one single-particle transition is strongly dominant. Assuming this to be the case and taking the values for $\nu p_{1/2} \rightarrow \pi s_{1/2}$ for $R=0,1$ and $\nu p_{1/2} \rightarrow \pi d_{3/2}$ for $R=2$ as the effective ones, we have

$$\begin{aligned} &\text{Rank 0}: \quad q_S \sim 0.92, \quad q_T \sim 1.08, \\ &\text{Rank 1}: \quad q_u \sim 0.47, \quad q_x \sim 0.64, \\ &\text{Rank 2}: \quad q_z \sim 0.71. \end{aligned}$$

The $R=0$ matrix elements. We first note that there does not seem to have been any recognition in publications dealing with the lead region that

$$1-q_S \approx -(1-q_T).$$

Secondly, because of the strong cancellation between the central and tensor components, it is vital to use a realistic interaction in the evaluation of q_S and q_T. For these reasons, the present results for the $R=0$ matrix elements are quite different from previous calculations or estimates. Comparison to experiment is difficult because one cannot disentangle quenching due to structure effects from that due to non-nucleonic effects, nor can one easily disentangle M_0^S from M_0^T.[2]

The $R=1$ matrix elements. The quenching of u is predicted to be ~40% greater than that of x. The contributions from the central part of the interaction are approximately equal but the tensor contribution to the quenching of u is large and the contribution to the quenching of x is small; hence, the stronger quenching of u. The present results are in quantitative agreement with semiempirical results of Damgaard, Broglia, and Riedal[34] and in poor agreement with the calculation of Ogawa and Arita[29] (who used the CAL interaction of Table III). We predict considerably less quenching than the estimates of Ejiri and Fujita.[11] Krmpotić, Ebert, and Wild[12] performed a detailed, erudite, and careful calculation of spin-dipole and beta-decay observables in the lead region. The results for 2p-2h quenching are not too different than the present ones for the $R=1$ matrix elements. Unfortunately, the residual interaction they used did not have an explicit tensor component and so the present results are to be preferred.

B. The $\nu 1g_{9/2} \rightarrow \pi 0h_{9/2}$ transition of Table V

We discuss these results separately from those of Table IV because they are atypical. A general difference is that the HO and WS results differ considerably more than for the results of Table IV. This difference can be traced to the $\nu 1g_{9/2} \rightarrow \pi 0h_{9/2}$ transitions themselves. As noted previously,[34] the $1g_{9/2}$ state has one radial node while the $0h_{9/2}$ state has none. Therefore there are two contributions of opposite sign to the radial integral and the value of the matrix element depends strongly on the position of the node. Thus, the WS and HO matrix elements differ considerably. The former are preferred.

A second difference is that the balance between the central and tensor contributions to the rank-zero matrix elements has changed relative to Table IV and now M_0^S is enhanced and M_0^T is quenched as in the case of $^{16}N(0^-) \rightarrow {}^{16}O(0^+)$ decay.[10]

Finally, the magnitude of x for this transition is about an order of magnitude below the mean value for the transitions of Table IV. Thus, there is potentially much more effect from 2p-2h admixtures. The small contribution from the central part of the interaction can be laid to a very large out-of-phase contribution from the $\nu 0i_{13/2} \rightarrow \pi 0j_{15/2}$ transition. In addition, the tensor contribution from this admixed transition is approximately equal to the total tensor contribution from all admixed transitions — of which there are 34.

TABLE VI. Contributions to the matrix element M_0^S from the possible single-particle transitions in $^{206}\mathrm{Tl}(0^-) \rightarrow ^{206}\mathrm{Pb}(0^+)$ β^- decay. The three interactions used are explained in the text. The matrix elements are in fm and were calculated with HO wave functions.

Orbit		Interaction		
ν	π	KH	$G_{\mathrm{H7B}} + G_{\mathrm{1p\text{-}1h}}$	$G_{\mathrm{H7B(central)}} + G_{\mathrm{1p\text{-}1h}}$
$2p_{1/2}$	$2s_{1/2}$	−6.546	−6.345	−6.341
$2p_{3/2}$	$1d_{3/2}$	−0.581	−0.622	−0.622
$1f_{5/2}$	$1d_{5/2}$	−0.506	−0.544	−0.544
$0i_{11/2}$	$0h_{11/2}$	+2.005	+1.944	+1.940
Total		−5.628	−5.567	−5.567

C. The tensor contribution to initial-state admixtures

We have emphasized the strong role of the tensor component of the residual interaction in final-state correlations for rank-zero and rank-one decays. The question arises as to the importance of the tensor component in initial-state admixtures. We investigated this effect by calculating the $^{206}\mathrm{Tl}(0^-) \rightarrow ^{206}\mathrm{Pb}(0^+)$ transition of Table II with the following three interactions: (a) The Kuo-Herling interaction for the orbits below ^{208}Pb truncated to the eight orbits below $Z = 82$, $N = 126$ shown in Fig. 1. The Kuo-Herling (KH) interaction in approximation (2) of Ref. 30 — which we used — has a bare G-matrix part and a 1p-1h renormalization part,

$$G_{\mathrm{KH}} = G_{\mathrm{bare}} + G_{\mathrm{1p\text{-}1h}}.$$

(b) The second interaction used replaced G_{bare} with G_{H7B}, which it is equivalent to in principle and closly equal to in fact. Thus,

$$G_2 = G_{\mathrm{H7B}} + G_{\mathrm{1p\text{-}1h}}.$$

This step was made so as to be able to separate the central and tensor components of G_{bare}. (c) Thus, the third interaction used was

$$G_3 = G_{\mathrm{H7B(central)}} + G_{\mathrm{1p\text{-}1h}}.$$

In all three cases the $\nu 1g_{9/2} \rightarrow \pi 0h_{9/2}$ transition was ignored and the $\nu 0i_{11/2} \rightarrow \pi 0h_{11/2}$ transition was added perturbatively using the H7B interaction with or without the tensor component as appropriate. The results are shown in Table VI. From comparison of the last two columns of Table VI we see that the tensor (and also LS) component of the interaction has negligible effect on the relative contributions of the different transitions. We conclude that — in this case at least — initial-state admixtures are insensitive to the tensor component of the interaction. This is not surprising since admixtures in the initial and final states are caused by different sets of two-body matrix elements.

D. Concluding remarks

The results presented here were motivated by a desire to understand first-forbidden beta decay in the A = 205–209 nuclei. They will be utilized in a study of this subject which is currently underway.[35] As stated above, the quenching of the rank-zero matrix elements is intricately intertwined with non-nucleonic effects and one cannot easily make a meaningful comparison of experiment with the present predictions; however, an attempt will be made.[35] The present results for the rank-one operators are quite consistent with a preliminary analysis[35] of the experimental data as well as with the semiempirical estimates of Damgaard, Broglia, and Riedel.[34] One should note that we have only dwelt on one aspect of the determination of the effective operators. We have assumed that initial-state admixtures can be handled within the model space. If not then their effect should also be included in the $q_\alpha(j_m \rightarrow j_i)$. We have not considered non-nucleonic effects such as mesonic processes and relativistic effects. Our point of view is that a careful appraisal of "final-state correlations" — which as shown can be quite sizable — will aid in the determination of these non-nucleonic effects.

ACKNOWLEDGMENTS

We thank I. S. Towner for a fruitful and educational correspondence. B. A. Brown provided the programming used in the extraction of two-particle matrix elements from the cited potentials. In addition, he provided the explanation (see Ref. 16) for the erroneous Eq. (8) of Ref. 1 and is also to be thanked for a reading of the manuscript. D. J. Millener provided valuable counsel. This research was supported by the U.S. Department of Energy under Contract No. DE-AC02-76CH00016.

[1] H. Sagawa and B. A. Brown, Phys. Lett. **143B**, 283 (1984).
[2] E. K. Warburton, J. A. Becker, B. A. Brown, and D. J. Millener, Ann. Phys. (N.Y.) **187**, 471 (1988).
[3] K. Kubodera, J. Delorme, and M. Rho, Phys. Rev. Lett. **40**, 755 (1978).
[4] P. A. M. Guichon, M. Giffon, J. Joesph, R. Laverrière, and C. Samour, Z. Phys. A **285**,183 (1978); P. A. M. Guichon, M. Giffon, and C. Samour, Phys. Lett. **74B**, 15 (1978).

[5]I. S. Towner, Comments Nucl. Part. Phys. **15**, 145 (1986).
[6]M. Kirchbach and M. Reinhardt, Phys. Lett. **208**, 79 (1988).
[7]A. Bohr and B. Mottelson, *Nuclear Structure* (Benjamin, New York, 1969, 1975), Vols. I and II.
[8]I. S. Towner, E. K. Warburton, and G. T. Garvey, Ann. Phys. (N.Y.) **66**, 674 (1971).
[9]I. S. Towner and J. C. Hardy, Nucl. Phys. **A179**, 489 (1972).
[10]I. S. Towner and F. C. Khanna, Nucl. Phys. **A372**, 331 (1981).
[11]H. Ejiri and J. I. Fujita, Phys. Rep. **38C**, 85 (1978).
[12]F. Krmpotic, K. Ebert, and W. Wild, Nucl. Phys. **A342**, 497 (1980).
[13]N. A. F. M. Poppelier and P. W. M. Glaudemans, Z. Phys. A **329**, 275 (1988).
[14]I. S. Towner, *A Shell Model Description of Light Nuclei* (Oxford University Press, Oxford, Great Britain, 1977).
[15]D. Zwarts and P. W. M. Glaudemans, Z. Phys. A **320**, 487 (1985).
[16]There is an unfortunate confusion in the literature concerning the 2p-2h effects of Eq. (4). In Ref. 1, our $\sum_{n,j} y_{nj,m_i}$ is referred to as α and the equation, Eq. (8), giving α is in error — a matrix element is missing from the denominator and the two-body matrix element is the wrong one for the process in question. Nevertheless, Sagawa and Brown calculated the quenching with the correct formula, namely, our Eq. (4). In their report on spin-dipole quenching in ^{40}Ca, Boucher and Castel (Ref. 17) also present the wrong formula for α since they show the same erroneous two-body matrix element [Eq. (5) of Ref. 17] as Eq. (8) of Ref. 1. Nevertheless, they also claim to have done the calculation correctly.
[17]P. M. Boucher and B. Castel, Phys. Rev. C **41**, 786 (1990); B. Castel (private communication).
[18]V. Gillet, A. M. Green, and E. A. Sanderson, Nucl. Phys. **88**, 321 (1966).
[19]A. Hosaka, K.-I. Kubo, and H. Toki, Nucl. Phys. **A244**, 76 (1985).
[20]M. Lacombe, B. Loiseau, J. M. Richard, R. Vinh Mau, J. Côté, P. Pirès, and R. de Tourreil, Phys. Rev. C **21**, 861 (1980).
[21]N. Anantaraman, H. Toki, and G. F. Bertsch, Nucl. Phys. **A398**, 269 (1983).
[22]G. Bertsch, J. Borysowicz, H. McManus, and W. G. Love, Nucl. Phys. **A284**, 399 (1977).
[23]The potential commonly designated "M3Y" in the literature uses the components labeled 1,4,7,8,11,14,16, and 18 in Table 1 of Ref. 22.
[24]T. Hamada and I. D. Johnston, Nucl. Phys. **34**, 382 (1962).
[25]R. Reid, Ann. Phys. (N.Y.) **50**, 411 (1968).
[26]The three symbols of the acronyms used in the literature for the potentials derived from nucleon-nucleon data conveys the origin (Hosaka, Paris, Michigan), the number of range parameters, and the type of form factor (one-boson-exchange, Yukawa).
[27]J. Streets, B. A. Brown, and P. E. Hodgson, J. Phys. G **6**, 839 (1983).
[28]D. Wang and M. T. McEllistrem, Phys. Rev. C **42**, 252 (1990).
[29]K. Ogawa and K. Arita, Nucl. Instrum. Methods **A271**, 280 (1988).
[30]T. T. S. Kuo and G. H. Herling, U.S. Naval Research Laboratory Report No. 2258, 1971 (unpublished).
[31]T. T. S. Kuo and G. E. Brown, Nucl. Phys. **85**, 40 (1966).
[32]B. Mottelson, private communication as quoted in Ref. 1.
[33]T. Suzuki, M. Oka, H. Hyuga, and A. Arima, Phys. Rev. C **26**,750 (1980).
[34]J. Damgaard, R. Broglia, and C. Riedel, Nucl. Phys. **A135**, 310 (1969).
[35]E. K. Warburton (unpublished).